

Effect of Limb Movements on Compact UWB Wearable Antenna Radiation Performance for Healthcare Monitoring

Richa Bharadwaj^{1, *}, Clive Parini², Shibhan K. Koul¹, and Akram Alomainy²

Abstract—This paper presents a detailed analysis of the human body limb movement influence on the radiation pattern of a wearable antenna during different activities. The analysis is carried out at 3, 6, 9 GHz of the 3–10 GHz UWB range of frequencies. Simulations are carried out on a human body model in CST microwave studio with a compact wearable antenna to obtain the body-worn antenna radiation patterns for lower and higher frequencies. This study gives an insight into the variation of the radiation patterns of a compact UWB antenna depending upon the position of the wearable antenna on the body. Results conclude that the radiation pattern of the wearable antenna changes significantly in terms of shape, size, level of distortion, and direction of maximum radiation with different limb movement activities and also depends upon the placement of the antenna on the limbs. The coverage area of the wearable antenna radiation pattern becomes highly directive and shrinks in coverage area for the shoulder/thigh node in comparison to the wrist/ankle wearable node by 10–15%. The bending of the limbs leads to deformation and reduction in area of the radiation pattern with values as high as 30–40% compared to free space scenario as the bending angle between the upper and lower arm/leg reduces. The analysis presented gives directional information regarding maximum radiation and the field strength of the radiation pattern for various activities performed. The present study reports results on the influence of the wearable antenna position, on detection and tracking performance of RF and microwave biomedical devices/sensors suitable for various healthcare applications such as tracking of human subject, patient monitoring, gait analysis, physical exercises, yoga, physiotherapy, and rehabilitation.

1. INTRODUCTION

Wearable devices have become an integral part of day-to-day life which is possible due to the miniaturization of circuitry and compact antennas leading to user-friendly portable Radio-Frequency (RF) and microwave medical devices. Wearable devices attract great interest in many day-to-day activities and constitute the core of several health monitoring applications [1–5]. For instance, wearable wireless tags can provide patient monitoring information which can help to prevent injury/assist in providing a person's location to relatives/doctor. The development of such remote health monitoring/personal healthcare devices requires an efficient system design and detailed analysis of the antennas used as the Transmitter/Receiver (Tx/Rx) node which reflect the system performance.

Impulse-Radio Ultra-Wideband (IR-UWB) has emerged as a promising solution for high resolution body centric communication applications [2–7]. It has become a very favourable technology for body area networks such as in-body, off-body, body-to-body and on-body links. UWB has attractive features such as low cost, high data rate, low power, easy implementation and low energy consumption [2–6], suitable

Received 14 December 2018, Accepted 2 February 2019, Scheduled 7 March 2019

* Corresponding author: Richa Bharadwaj (richabharadwaj@hotmail.com, richa_b@care.iitd.ac.in).

¹ Microwave and RF Group, Centre for Applied Research in Electronics, Indian Institute of Technology Delhi, New Delhi 110016, India. ² Antennas and Electromagnetics Group, School of Electronic Engineering and Computer Science, Queen Mary University of London, London E1 4NS, UK

for applications in the field of sports, medical, entertainment and military where the human body is an integral part. Antenna is a key component in body centric communications, and its performance can vary significantly for different body postures, limb movements, and distances from the body surface [6, 8–10]. A number of studies and research work have focused on body-centric channel measurements, modelling and characterisation leading to detailed investigation of the links formed in terms of classifying line-of-sight (LOS), non-line of sight (NLOS) or partial NLOS channels [6, 9–13]. Work related to analysis of on-body channel has been carried out in [9–12] and for off-body in [6, 13] where several nodes over whole body have been studied, and best/worst links have been identified. Most common links studied for body-centric communication are wrist and torso regions which are chosen due to the feasibility of placement of probable wearable devices and user convenience. Coplanar waveguide (CPW) fed UWB planar antennas are compact, low cost, easy to fabricate, easily integrated with wireless systems and are frequently used for wearable communication for various WBAN applications [6, 13–19]. In [6] compact tapered slot antennas are used for high accuracy limb tracking and human 3D localisation. In [14] small CPW-fed monopole UWB antennas are used for footwear body area network telemetry. A compact CPW-fed planar monopole UWB antenna has been designed for UWB cancer detection systems in [16]. Thus, a compact tapered slot CPW-fed UWB wearable antenna [6, 10] is chosen for the radiation pattern analysis during limb movement activities.

To a great extent the radiation patterns of the wearable antenna determine the behaviour of an antenna for free space or body worn scenarios. In most of the UWB channel link studies, 3D/2D radiation patterns are often overlooked, which play an important role in the channel link type and further processing of data depending upon intended application. Generally only the torso region of the human subject is considered to obtain simulated/measured wearable antenna radiation patterns [10, 20, 21]. Some preliminary work related to body worn antenna radiation patterns has been carried out in [22] and [23] showing variation in the radiation patterns performance. Hence, it is imperative to study the radiation patterns of the wearable antenna for different prospective body locations and activities to get a deeper understanding of the propagation phenomenon between two or more nodes present in a body area network.

The wearable antenna radiation pattern plays a significant role in the overall performance of the RF and microwave wearable medical device/sensor for healthcare sensing and monitoring applications, hence, is the main objective of the work presented. Variation of the radiation pattern performance and analysis for different locations of the antenna on the body for various limb movement activities is reported for the first time, addressing the gap of understanding the influence of wearable antennas on the propagation phenomenon. This paper presents 3D and 2D radiation pattern analysis for a compact UWB wearable antenna for various body locations and limb movements through numerical investigations. The limb movement postures chosen are common activities performed during physical exercises, physiotherapy and rehabilitation. The wearable antenna is placed on various joints of the limbs (arms and legs) leading to variation in the antenna orientation causing change in the radiation pattern.

The paper is organized as follows. In Section 2, the details of the human body model are provided, which is simulated in Computer Simulation Technology Microwave Studio (CST MWS), and the description of the design parameters of the chosen wearable antenna is presented. In Section 3, analysis is provided of the radiation patterns observed for different limb movement postures and reason behind the behavior of the pattern for each limb movement carried out. Finally, the conclusion is drawn in Section 4.

2. NUMERICAL MODELLING AND METHODOLOGY

A human body model is designed using CST Microwave Studio. A schematic of the human body model in sitting position is presented in Fig. 1(a). The analysis is carried out at 3, 6, 9 GHz of the 3–10 GHz UWB range, and sine modulated Gaussian pulse is used for signal transmission. The body material comprises bone, fat, muscle, and skin, and the weights assigned to calculate weighted average of the dielectric permittivity and conductivity are: 10% skin, 30% fat, 40% muscle, and 20% bone (average of bone cancellous, bone cortical and bone marrow), resulting in a weighted averaged relative permittivity of 25.87 and conductivity of 3.14 S/m at 6.5 GHz [24, 25]. The height of the human body is 1.72 m and

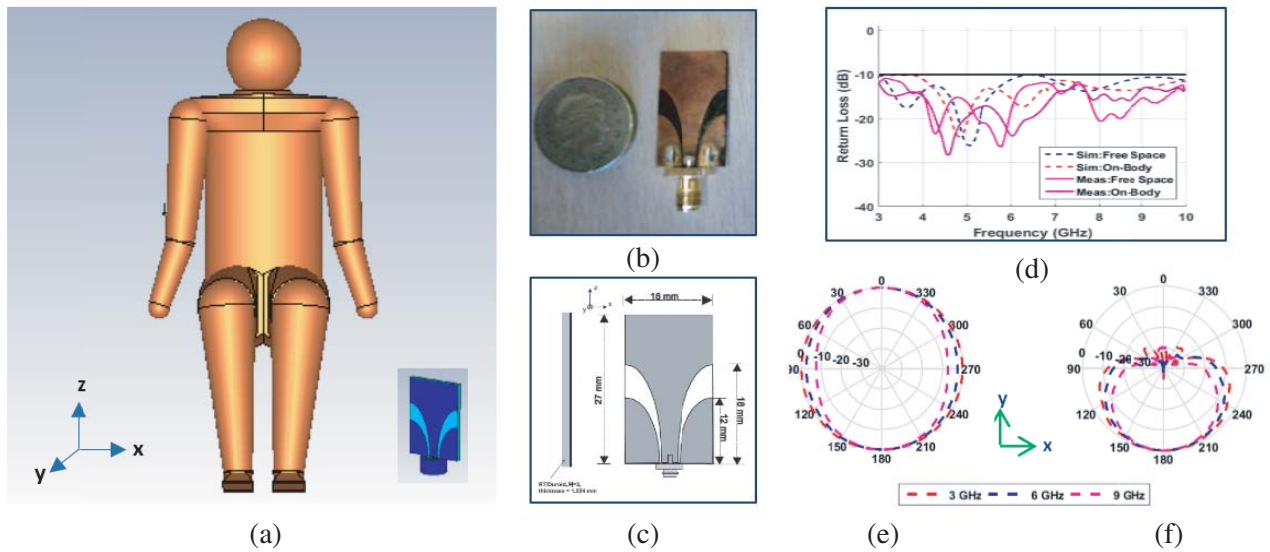


Figure 1. (a) Human body model schematic with average built and height in sitting position and compact tapered slot UWB antenna shown in inset. (b) Fabricated TSA Antenna. (c) TSA antenna schematic and dimensions. (d) Simulated and measured return loss for free space and on-body scenario. The TSA antenna azimuth radiation pattern for 3, 6, 9 GHz when in (e) free space scenario and (f) when placed on the human body model.

Table 1. Human model dimensions.

Human Body Dimensions (cm)			
Height	172	Waist	86
Upper Arm Length	35	Upper Leg Length	46
Forearm Length	25	Shank Length	45
Shoulder Circumference	35	Thigh Circumference	70
Elbow Circumference	25	Knee Circumference	50
Wrist Circumference	18	Ankle Circumference	25

has average built. The dimensions of the human subject are presented in Table 1, which are in line with the dimensions of an average built male human.

A compact and low cost tapered slot antenna (TSA) [6, 10] is chosen in this study (Fig. 1(a) inset: Simulated, Fig. 1(b): Fabricated and Fig. 1(c): Dimensions of the antenna) which has been used in various domains of the body centric channel modelling and applications such as localisation, tracking, and target detection, hence, has proved to be very suitable for PAN/WBAN short-range communication in terms of performance and fidelity. The TSA antenna has excellent impedance matching with return loss below -10 dB (Fig. 1(d)) and radiation performance (Fig. 1(e): Free Space and Fig. 1(f): On-Body) in the UWB range with relatively constant gain across the whole frequency band. The total antenna size is $27\text{ mm} \times 16\text{ mm}$. The TSA antennas are used as wearable devices which are placed around 2 to 3 mm away from the human body surface. The wearable antennas are placed on different locations of the arm (shoulder (S1)/elbow (S2)/wrist (S3)) and leg (thigh (S4)/knee (S5)/ankle (S6)). The upper limbs are moved in sideways and forward directions at intervals of 30 degrees, with total of 5 positions. The lower limbs are moved in sideways/forward/backward directions at intervals of 30 degrees for 3 positions. Apart from limb movement, the effect of variation in limb bending is also studied by placing the antennas on the wrist/elbow and ankle/knee for arms and legs respectively.

3. ANTENNA RADIATION PATTERNS

The radiation patterns were simulated for each wearable antenna location and limb positions. Due to the presence of the body and proximity of the antenna to it, there is variation of the radiation pattern in terms of directivity in comparison to the scenario when no-body is present which is clearly depicted in Figs. 1(e) and (f). It can be observed that the directivity increases for all the cases as the front-to-back ratio of the radiation pattern is significantly increased due to high reflections from the body at these frequencies caused by increase in conductivity [10, 23]. A detailed analysis of the radiation pattern for different locations and limb movements is given below for 3/6/9 GHz. The limb movement activities in various directions are a common routine followed in day-to-day life and also for healthcare/sports monitoring activities with wearable devices attached, hence are important to study the behavior of the variation in antenna radiation for such movements. The investigation carried out is suitable for various body worn antennas having similar characteristics and antenna performance.

3.1. Sideways Arm Movement

Figure 2 shows the human model schematic in sitting posture and the 3D radiation pattern (x - z and x - y plane at 3 GHz) for 90 degrees position of the right arm for the antenna placed on the shoulder. The sideways arm angle is measured with respect to the torso and the shoulder region. The 3D radiation pattern directly shows the direction and region of maximum radiation strength when the wearable antenna is placed on the shoulder region of the arm.

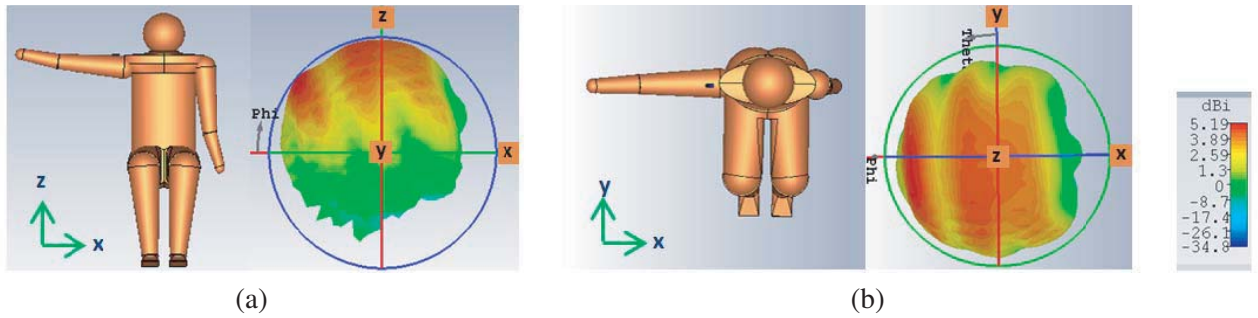


Figure 2. Human body model schematic in sitting position performing upper right limb sideways movement: 90 degrees (shoulder: 3 GHz). (a) X - Z plane, (b) X - Y plane.

Detailed 2D polar plot of the radiation patterns for the three joints: shoulder, elbow, and wrist for various positions and frequency are shown in Fig. 3 and Fig. 4 for the x - z plane and x - y plane, respectively. Different positions of the arm (0° , 30° , 60° , 90° , 120°) and frequencies lead to modification in the antenna radiation pattern performance in terms of direction of maximum radiation, radiation strength and coverage area (2D polar plot). For each body-worn position when the frequency is increased from ($3 \rightarrow 6 \rightarrow 9$ GHz), the coverage area of the radiation pattern decreases which is depicted in Fig. 3(a). The coverage area decreases by 10–20%, 25–30% and 30–40% for 3/6/9 GHz, respectively, compared with free space radiation patterns. As the frequency is increased from ($3 \rightarrow 6 \rightarrow 9$ GHz), the coverage area of the radiation pattern decreases. With the increase of frequency, the electric length gets reduced; the antenna becomes electrically large to some extent at the higher frequencies; more edge reflections are created leading to more directive patterns.

As observed in Fig. 4, the arm positions 0 and 30 degrees follow similar radiation pattern trend, and 90/120 degree arm positions have similar radiation pattern to the overall pattern shifting towards the right in the x - y plane. For 90 and 120 degrees, there is more distortion of the radiation pattern due to the position of the arm leading to deviation in radiation pattern trend followed by the lower angle arm position. There is more variation in the radiation pattern plot for 9 GHz frequency than 3 or 6 GHz frequency which can be observed in Fig. 4(a). As the coverage area for the 9 GHz radiation pattern is least, the variation for different limb positions is more prominent than the lower frequencies such as

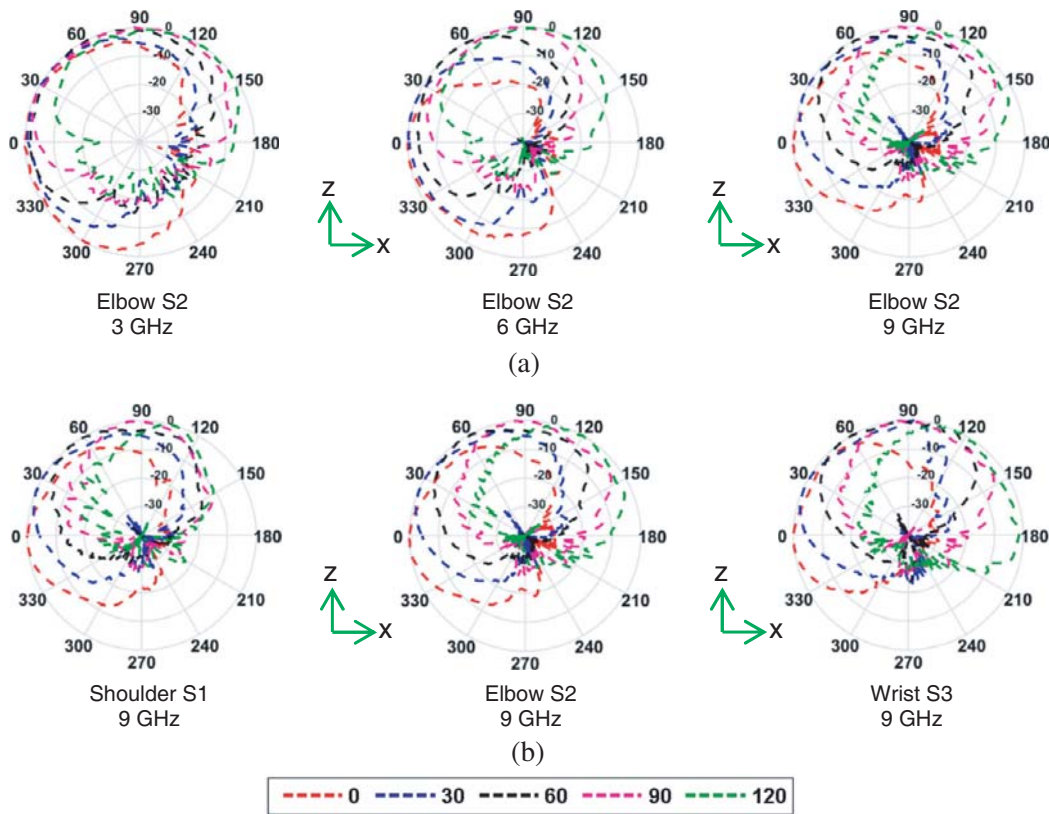


Figure 3. X-Z plane normalized radiation plots for (a) different frequencies (3/6/9 GHz): elbow, (b) same frequency (9 GHz): wrist. Sideways arm position: 0° to 120°.

Table 2. HPBW: Sideways arm movement activity (varied frequency).

X-Z plane: Arm Position Angle (0° → 120°)		X-Y plane: Arm Position Angle (0° → 60°/90° → 120°)	
Antenna Location	HPBW	Antenna Location	HPBW
3 GHz: Elbow (S2)	100°–140°	3 GHz: Elbow (S2)	120°–140°/100°–110°
6 GHz: Elbow (S2)	55°–85°	6 GHz: Elbow (S2)	110°–120°/80°–90°
9 GHz: Elbow (S2)	40°–60°	9 GHz: Elbow (S2)	70°–100°/45°–65°

3 GHz chosen which have wider coverage area. For Fig. 4(a), the coverage area decreases in the *x-y* plane by 10–20%, 10–25% and 10–30% for 3/6/9 GHz, respectively, keeping the free space radiation patterns as reference. Arm positions, 60 and 90 degrees, have higher coverage area of the radiation pattern contour, and 0 degree position has minimum coverage area due to the orientation of the wearable antenna and the respective arm position. As observed in Fig. 4(b), the shoulder region leads to smaller radiation patterns than the wrist region, due to the variation in size of the arm. Hence, the shoulder region has less spread of the radiation pattern contour, which increases further for the elbow region and maximum coverage area obtained for the wrist region. Half power beamwidth (HPBW) range of values for each antenna location corresponding to Fig. 3(a) and Fig. 4(a) is presented in Table 2. The HPBW values indicate reduction from 3 → 9 GHz frequency due to the directive nature of the antenna at higher frequencies. HPBW values for 9 GHz for the corresponding radiation patterns in Fig. 3(b) and Fig. 4(b) are presented in Table 3. The antenna placed on the shoulder has minimum HPBW values in comparison to body-worn antenna placed on the wrist.

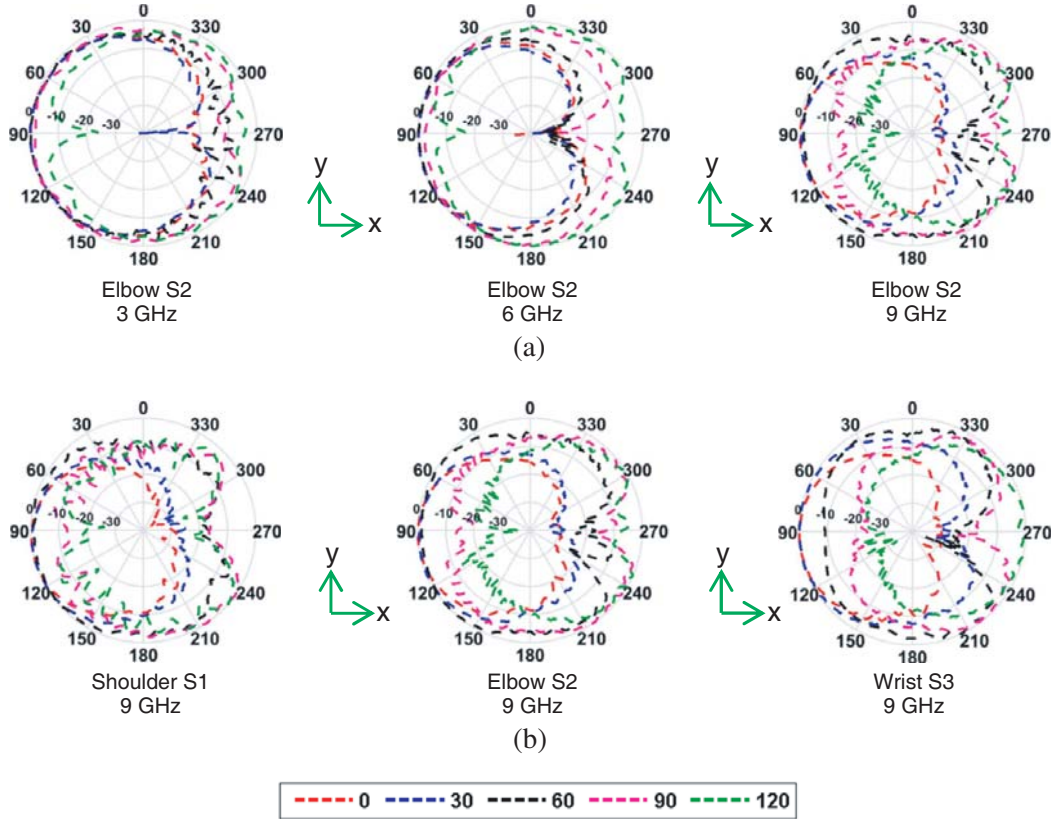


Figure 4. X-Y plane normalized radiation plots for (a) different frequencies (3/6/9 GHz): elbow, (b) same frequency (9 GHz): shoulder/elbow/wrist. Sideways arm position: 0° to 120° .

Table 3. HPBW: Sideways arm movement activity (same frequency).

X-Z plane: Arm Position Angle ($0^\circ \rightarrow 120^\circ$)		X-Y plane: Arm Position Angle ($0^\circ \rightarrow 60^\circ/90^\circ \rightarrow 120^\circ$)	
Antenna Location	HPBW	Antenna Location	HPBW
9 GHz: Shoulder (S1)	$25^\circ\text{--}40^\circ$	9 GHz: Shoulder (S1)	$65^\circ\text{--}90^\circ/40^\circ\text{--}60^\circ$
9 GHz: Elbow (S2)	$40^\circ\text{--}60^\circ$	9 GHz: Elbow (S2)	$70^\circ\text{--}100^\circ/45^\circ\text{--}65^\circ$
9 GHz: Wrist (S3)	$45^\circ\text{--}75^\circ$	9 GHz: Wrist (S3)	$75^\circ\text{--}110^\circ/50^\circ\text{--}85^\circ$

3.2. Forward Arm Movement

Figure 5 presents human model schematic and 3D antenna radiation pattern for (x - z and x - y plane at 3 GHz) for 60 degree position of the right arm for the antenna placed on the wrist. The forward arm angle is to the torso and shoulder region. Detailed plot of the 2D radiation patterns for the three joints: wrist, elbow, and shoulder for various positions (0° , 30° , 60° , 90° , 120°) and frequency are shown in Fig. 6 and Fig. 7 for the x - z plane and x - y plane, respectively.

There is not much variation in the radiation patterns in the x - y or x - z plane when the human arm is performing forward movement which is dependent on the position and orientation of the wearable antenna on the arm. As the displacement is taking place in the y - z plane of the simulation volume, x - z plane does not depict the variation in main lobe direction with changing arm position. If the wearable antenna was placed over the front region of the arm instead of the side of the arm (as seen in Fig. 5), main lobe direction variation will be more prominent in the y - z plane.

Till 30 degrees the antenna is in close proximity with the human body due to the position of the

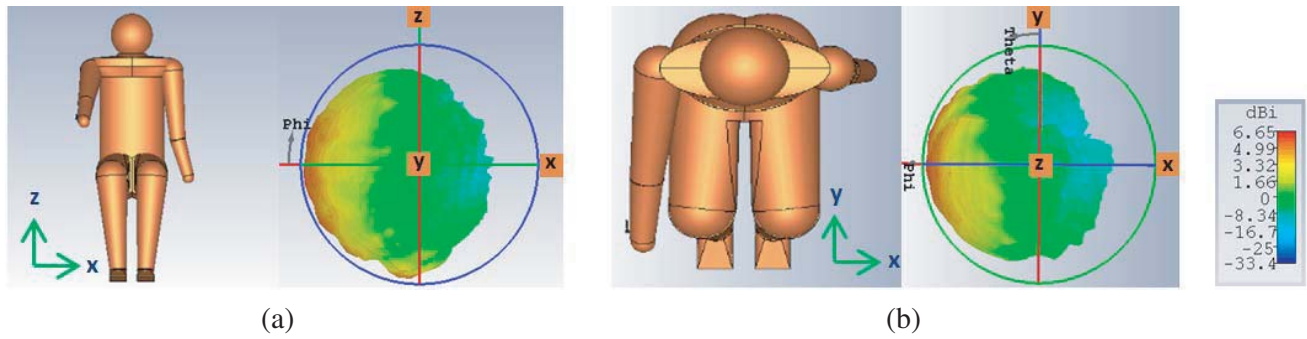


Figure 5. Human body model schematic in sitting position performing upper right limb forward movement: 60 degrees (wrist: 3 GHz). (a) X-Z plane, (b) X-Y plane.

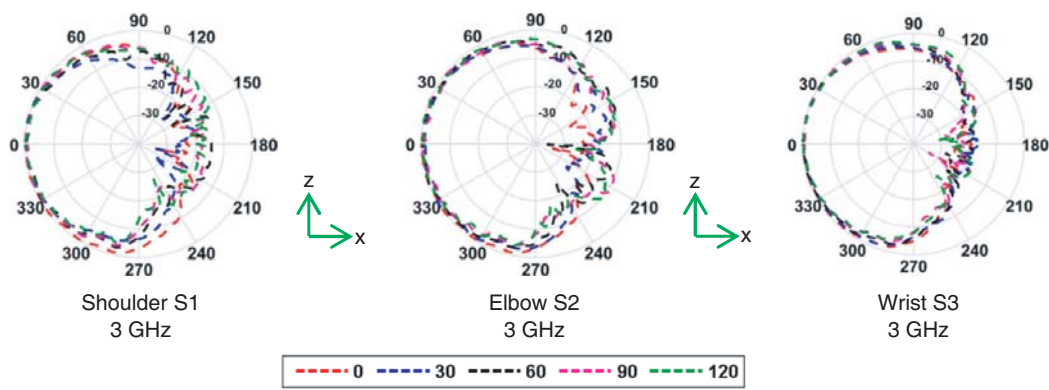


Figure 6. X-Z plane radiation plots for: Same frequency (3 GHz): shoulder/elbow/wrist. Forward arm position: 0° to 120°.

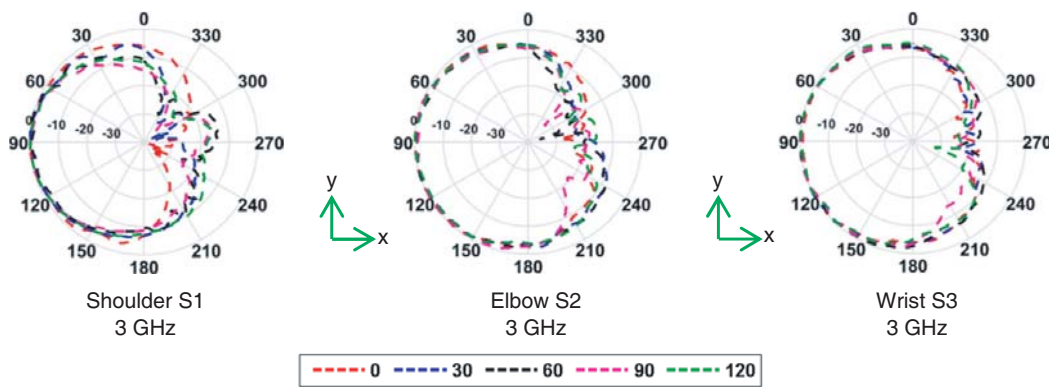


Figure 7. X-Y plane normalized radiation plots for: Same frequency (3 GHz): shoulder/elbow/wrist. Forward arm position: 0° to 120°.

arm for the elbow and wrist joints. This leads to larger effect of the human torso region on the radiation pattern of the wearable antenna. After 30 degrees there is significant role of the arm structure and not the human torso/thigh region in the formation of the radiation pattern of the wearable antenna as the arm is moving further from the torso/thigh region. For the shoulder joint the variation is not much as the human torso is always in close proximity with the antenna location. For the wrist, the case is different as it displaces maximum from the torso region of the body. From Figs. 6 and 7 it can be observed that the coverage area of the wrist is larger than the shoulder or elbow as it depends on how

much radiation is absorbed by the body mass in proximity with the antenna. As seen in Fig. 6, for x - z plane, the coverage area reduces by 10–25%, 5–10%, 5–10% for shoulder/elbow/wrist respectively when compared with free space radiation pattern at 3 GHz. For x - y plane the coverage area reduces by 25–30%, 20–25%, 15–20% for shoulder/elbow/wrist respectively.

HPBW range of values for each antenna location at 3 GHz corresponding to Fig. 6 and Fig. 7 is presented in Table 4. The HPBW values show lower magnitude for shoulder region in comparison to the wrist due to the proximity of the wearable antenna with the higher body volume and the vicinity of the torso region.

Table 4. HPBW: Forward arm movement activity.

X-Z plane: Arm Position Angle ($0^\circ \rightarrow 120^\circ$)		X-Y plane: Arm Position Angle ($0^\circ \rightarrow 120^\circ$)	
Antenna Location	HPBW	Antenna Location	HPBW
3 GHz: Shoulder (S1)	85° – 115°	3 GHz: Shoulder (S1)	75° – 100°
3 GHz: Elbow (S2)	120° – 140°	3 GHz: Elbow (S2)	110° – 140°
3 GHz: Wrist (S3)	130° – 150°	3 GHz: Wrist (S3)	120° – 150°

3.3. Sideway/Forward/Backward Leg Movement

The forward and backward leg movement shows a similar trend to that of the forward arm movement as the placement of the wearable antennas is the same as that of the arms which is facing side outwards as shown in Fig. 5 and Fig. 8. For the leg movement, the lower torso/thigh region is considered as reference to measure the angles. The sideways movement of the leg with antennas located at a similar position to that of forward/backward leg movement will lead to variation in the direction of the radiation pattern in the x - z plane. The leg is moved in forward, backward, and sideways directions with an interval of 30 degrees in each direction. Figs. 8 and 9 show sample plots in 2D and 3D, respectively, for forward leg movement at 3 GHz frequency in the x - z and x - y planes. From the 3D plot of the forward leg movement, it can be clearly observed that the position of the leg and location of the wearable antenna directly influence the radiation pattern behavior. The main variation in the radiation pattern of the wearable antenna is the coverage area and maximum lobe direction in the radiation pattern. In comparison to the shoulder/wrist, there is significant reduction (10–15%) in the radiation pattern area for the antenna placed on the thigh/ankle region. For the ankle, the reduction in coverage area is noticeable compared to the wrist. HPBW range of values for each antenna location at 3 GHz corresponding to Fig. 9 is presented in Table 5. The HPBW values show lower magnitude for the thigh region than the ankle due to the proximity of the wearable antenna with the higher body volume and the proximity of the torso region. The main cause of reduction in coverage area/HPBW is the larger diameter and thickness of the legs in comparison to the arm.

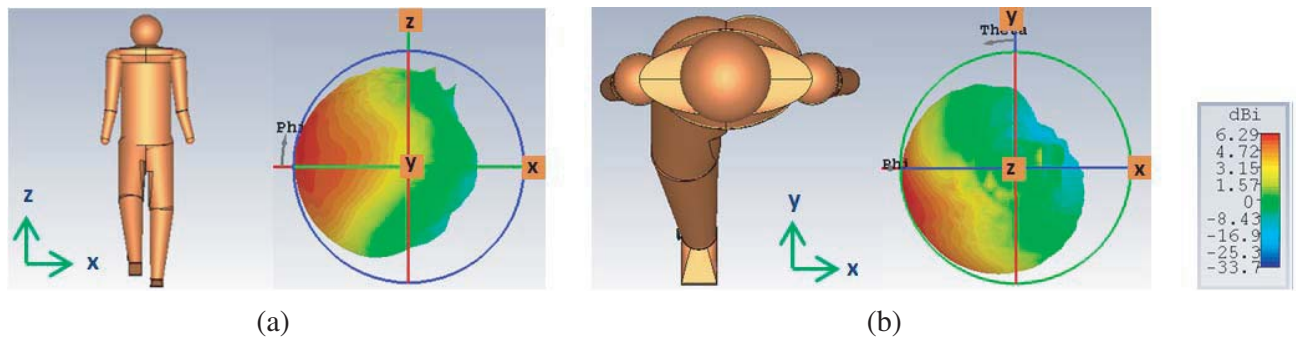


Figure 8. Human body model schematic in standing position performing lower right limb forward movement: 30 degrees (wrist: 3 GHz). (a) X-Z plane, (b) X-Y plane.

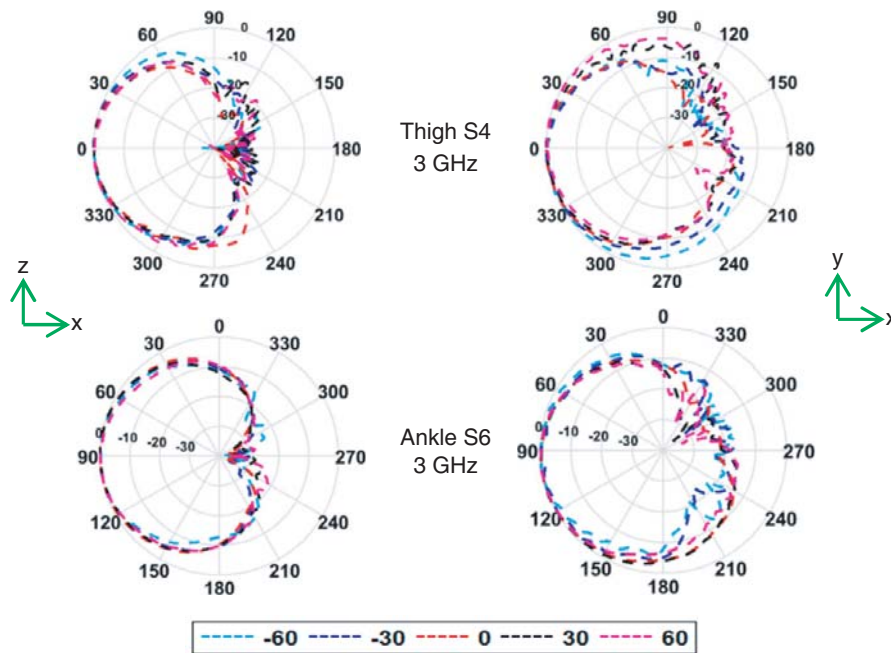


Figure 9. X-Z and X-Y plane normalized radiation pattern for 3 GHz frequency, forward leg movement for thigh/ankle. Ankle. Forward and backward leg position: -60° to 60° .

Table 5. HPBW: Forward and backward leg movement activity.

X-Z plane: Leg Position Angle ($-60^\circ \rightarrow 60^\circ$)		X-Y plane: Leg Position Angle ($-60^\circ \rightarrow 60^\circ$)	
Antenna Location	HPBW	Antenna Location	HPBW
3 GHz: Thigh (S4)	$50^\circ-90^\circ$	3 GHz: Thigh (S4)	$70^\circ-90^\circ$
3 GHz: Ankle (S6)	$80^\circ-100^\circ$	3 GHz: Ankle (S6)	$95^\circ-110^\circ$

3.4. Limb Bending

Radiation patterns have also been analyzed for upper and lower limbs bending which significantly vary with antenna orientation and bending angle. Limb bending is another common activity performed during physical exercises, rehabilitation, and physiotherapy. It gives indication regarding the flexibility and range of movement of the elbow and knee joint. By placing antennas/wearable devices on various joints, one can monitor the limb bending progress and performance. The antenna is placed on the wrist/ankle and elbow/knee for studying the sideways arm and backward leg bending scenarios. For the limb bending activity, the arm/leg at 180 degree vertical position is considered as reference for the measured angles. The angle formed between the upper and lower regions of the arm/leg is the bending angle.

The 3D radiation pattern for $x-z$ and $x-y$ plane view showing 30 degrees arm bend is presented in Fig. 10. It can be observed that the 3D radiation pattern is more distorted for the limb bending activity than simple limb forward/sideways/backward movements. As the arm is bent from 180 to 30 degrees (Fig. 11), distortion of the radiation pattern starts to take place near 120 degree bend of the forearm for the antenna placed on the wrist. For the antenna placed on the elbow distortion of the pattern takes place near 90 degree bend.

The distortion is observed in both $x-z$ and $x-y$ planes of the radiation pattern 3D/2D plots. The distortion is mainly caused due to the proximity of the upper/fore arm with the antenna when placed on the wrist/elbow as the bending angle decreases, which acts as an obstruction for the radiating region

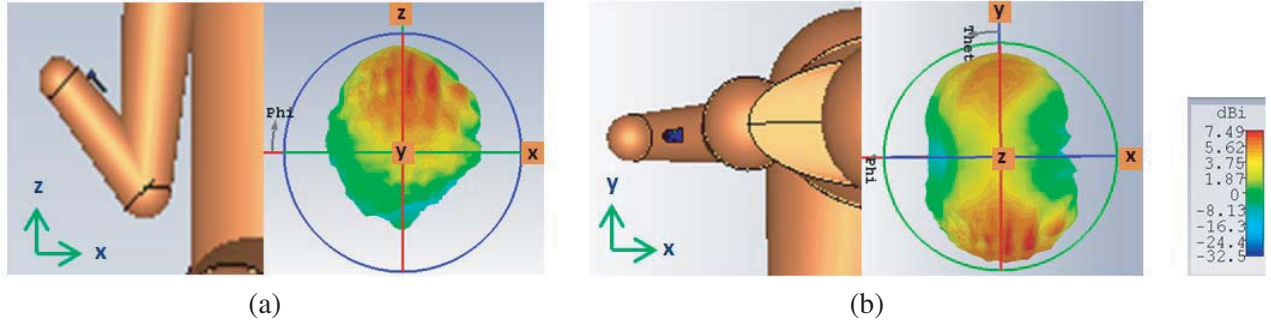


Figure 10. Human arm model schematic performing right arm sideways bending movement at 30 degrees (wrist: 3 GHz). (a) X-Z plane, (b) X-Y plane.

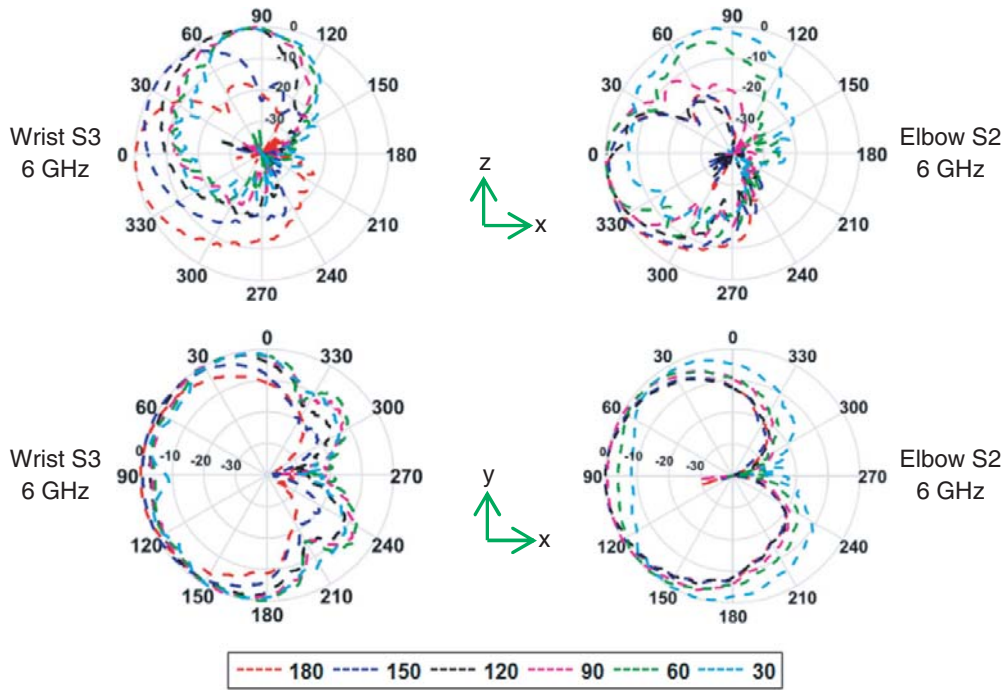


Figure 11. Arm bending activity: X-Z and Y-Z plane normalized radiation pattern for 6 GHz frequency: wearable antenna placed on wrist and elbow performing limb bending movement (180 to 30 degrees angle between the forearm and the upper arm).

of the antenna. The leg bending activity considers five positions of the leg from 180 degrees to 30 degrees bending angle between the upper and lower leg. For the backward leg movement, the radiation patterns for the antenna nodes also incur distortion especially after 60 degree angle. The reason for distorted radiation patterns of the body-worn antennas placed on the back region of the ankle and knee is the vicinity of the upper leg and lower leg during limb bending activity. Maximum distortion is observed when minimum possible bending angle is formed between the upper and lower arm/leg which in the current study is 30 degrees. This can be clearly seen from the radiation pattern plots presented in Fig. 11 for the arm bending activity at 6 GHz. For the x - z plane, a reduction in coverage area by 15–25%, 30–40% and 30–45% is observed for 3/6/9 GHz, respectively. For the x - y plane, a reduction in coverage area of the radiation patterns by 10–25%, 15–30% and 15–35% is observed for 3/6/9 GHz, respectively. The HPBW for arm bending movement is presented in Table 6. The main cause of reduction in coverage area/HPBW is the bending of the limbs which leads to more directive radiation patterns.

Table 6. HPBW: Arm bending activity.

X-Z plane: Bending Angle ($180^\circ \rightarrow 30^\circ$)		X-Y plane: Bending Angle ($180^\circ \rightarrow 30^\circ$)	
Antenna Location	HPBW	Antenna Location	HPBW
6 GHz: Elbow (S2)	$35^\circ\text{--}55^\circ$	6 GHz: Elbow (S2)	$55^\circ\text{--}95^\circ$
6 GHz: Wrist (S3)	$40^\circ\text{--}65^\circ$	6 GHz: Wrist (S3)	$65^\circ\text{--}95^\circ$

4. CONCLUSION

In this paper the effect of limb movement on the wearable antenna radiation pattern performance for various optimal limb locations has been investigated in the UWB frequency range. Results show reduction in radiation pattern coverage area (2D polar plots) for the shoulder/thigh region by 10–15% in comparison to the wrist/ankle region during limb movement. The HPBW ranges from (3 GHz: $75^\circ\text{--}100^\circ/70^\circ\text{--}90^\circ$ X-Y plane) for shoulder/thigh region compared with wrist/ankle region (3 GHz: $120^\circ\text{--}150^\circ/95^\circ\text{--}110^\circ$ X-Y plane). This is because the bulk of the human body is close to the wearable antenna for the shoulder/thigh region whereas for the wrist/ankle region, the body is reduced to the mass mainly present on the wrist/ankle. The main lobe direction changes for the antennas placed on the arm/legs during various movements and is dependent on the direction of limb movement with maximum variation observed for the wrist/ankle region. It can be observed that the radiation pattern reduces in coverage area/HPBW from 3 GHz to 9 GHz (HPBW: $100^\circ\text{--}140^\circ \rightarrow 40^\circ\text{--}60^\circ$) leading to more directive patterns with max reduction in coverage area by 20% to 40% respectively when compared with free space patterns. The bending of the limbs leads to modification of the radiative behavior (high distortion and variation in directivity) of the antenna especially for 60/30 degrees arm or leg bend with HPBW as low as $35^\circ\text{--}40^\circ$ (6 GHz) for X-Z plane and $55^\circ\text{--}65^\circ$ (6 GHz) for X-Y plane. The analysis and evaluations of the wearable antenna radiative behaviour during limb movement activities provides deeper insight on how the wearable antenna position influence the communication links which is much needed to design efficient RF and microwave biomedical devices for detection, sensing, tracking and monitoring purpose.

REFERENCES

1. Chahat, N., M. Zhadobov, R. Sauleau, and K. Ito, "A compact UWB antenna for on-body applications," *IEEE Trans. on Antennas and Propag.*, Vol. 59, No. 4, 1123–1131, April 2011.
2. Abbasi, Q. H., M. Ur Rehman, K. Qaraqe, and A. Alomainy, *Advances in Body-centric Wireless Communication: Applications and State-of-the-art*, IET publication, 2016.
3. Hall, P. S. and Y. Hao, "Antennas and propagation for body centric communications," *2006 First European Conf. on Antennas and Propag.*, 1–7, Nice, 2006.
4. Yang, X., et al., "Monitoring of patients suffering from REM sleep behavior disorder," *IEEE Journal of Electromagnetics, RF and Microwaves in Medicine and Biology*, Vol. 2, No. 2, 138–143, Jun. 2018.
5. Alemarveen, A., S. Noghianian, and R. Fazel-Rezai, "Antenna effects on respiratory rate measurement using a UWB radar system," *IEEE Journal of Electromagnetics, RF and Microwaves in Medicine and Biology*, Vol. 2, No. 2, 87–93, Jun. 2018.
6. Bharadwaj, R., S. Swaisaenyakorn, C. G. Parini, J. C. Batchelor, and A. Alomainy, "Impulse radio ultra-wideband communications for localization and tracking of human body and limbs movement for healthcare applications," *IEEE Trans. on Antennas and Propag.*, Vol. 65, No. 12, 7298–7309, Dec. 2017.
7. Abbasi, Q. H., et al., "Ultrawideband band-notched flexible antenna for wearable applications," *IEEE Antennas and Wireless Propag. Lett.*, Vol. 12, 1606–1609, 2013.
8. Khaleel, H. R., H. M. Al-Rizzo, D. G. Rucker, and S. Mohan, "A compact polyimide-based UWB antenna for flexible electronics," *IEEE Antennas and Wireless Propag. Lett.*, Vol. 11, 564–567, 2012.

9. Smith, D. B., D. Miniutti, T. A. Lamahewa, and L. W. Hanlen, "Propagation models for body-area networks: A survey and new outlook," *IEEE Antennas Propag. Mag.*, Vol. 55, No. 5, 97–117, Oct. 2013.
10. Alomainy, A., A. Sani, A. Rahman, J. G. Santas, and Y. Hao, "Transient characteristics of wearable antennas and radio propagation channels for ultrawideband body-centric wireless communications," *IEEE Trans. on Antennas and Propag.*, Vol. 57, No. 4, 875–884, Apr. 2009.
11. Abbasi, Q. H., A. Sani, A. Alomainy, and Y. Hao, "Experimental characterization and statistical analysis of the pseudo-dynamic ultrawideband on-body radio channel," *IEEE Antennas and Wireless Propagation Letters*, Vol. 10, 748–751, 2011.
12. Kumpuniemi, T., M. Hamalainen, K. Y. Yazdandoost, and J. Iinatti, "Categorized UWB on-body radio channel modeling for WBANs," *Progress In Electromagnetics Research B*, Vol. 67, 1–16, 2016.
13. Pasquero, O. P. and R. D'Errico, "A spatial model of the UWB off-body channel in indoor environments," *IEEE Transactions on Antennas and Propagation*, Vol. 64, No. 9, 3981–3989, Sept. 2016.
14. Gaetano, D., P. McEvoy, M. J. Ammann, J. E. Browne, L. Keating, and F. Horgan, "Footwear antennas for body area telemetry," *IEEE Transactions on Antennas and Propagation*, Vol. 61, No. 10, 4908–4916, Oct. 2013.
15. Liu, J., S. Zhong, and K. P. Esselle, "A printed elliptical monopole antenna with modified feeding structure for bandwidth enhancement," *IEEE Transactions on Antennas and Propagation*, Vol. 59, No. 2, 667–670, Feb. 2011.
16. Jafari, H. M., M. J. Deen, S. Hranilovic, and N. K. Nikolova, "A study of ultrawideband antennas for near-field imaging," *IEEE Transactions on Antennas and Propagation*, Vol. 55, No. 4, 1184–1188, Apr. 2007.
17. Gogoi, P. J., S. Bhattacharyya, and N. S. Bhattacharyya, "CPW-fed body worn monopole antenna on magneto-dielectric substrate in C-band," *Progress In Electromagnetics Research B*, Vol. 84, 201–213, 2018.
18. Nejatijahromi, M., M. Naghshvarianjahromi, and M. U. Rahman, "Compact CPW fed switchable UWB antenna as an antenna filterat narrow-frequency bands," *Progress In Electromagnetics Research B*, Vol. 81, 119–209, 2018.
19. Yan, S., L. A. Y. Poffelie, P. J. Soh, X. Zheng, and G. A. E. Vandenbosch, "On-body performance of wearable UWB textile antenna with full ground plane," *2016 10th European Conference on Antennas and Propagation (EuCAP)*, 1–4, Davos, 2016.
20. Yimdjo Poffelie, L. A., P. J. Soh, S. Yan, and G. A. E. Vandenbosch, "A high-fidelity all-textile UWB antenna with low back radiation for off-body WBAN applications," *IEEE Transactions on Antennas and Propagation*, Vol. 64, No. 2, 757–760, Feb. 2016.
21. Catherwood, P. A., S. S. Bukhari, G. Watt, W. G. Whittow, and J. McLaughlin, "Body-centric wireless hospital patient monitoring networks using body-contoured flexible antennas," *IET Microwaves, Antennas & Propagation*, Vol. 12, No. 2, 203–210, Jul. 2, 2018.
22. Yang, W. B. and K. Sayrafian, "Radiation pattern of an UWB wearable antenna: A preliminary study," *7th Int. Conf. on Body Area Networks*, Oslo, Norway, Sept. 24–26, 2012.
23. Bharadwaj, R., C. Parini, and A. Alomainy, "Experimental investigation of 3-D human body localization using wearable ultra-wideband antennas," *IEEE Trans. Antennas Propag.*, Vol. 63, No. 11, 5035–5044, Nov. 2015.
24. Rehman, M. U., Y. Gao, X. Chen, C. G. Parini, and Z. Ying, "Effects of human body interference on the performance of a GPS antenna," *The Second European Conf. on Antennas and Propag., EuCAP 2007*, 1–4, Edinburgh, 2007.
25. Bharadwaj, R., A. Alomainy, and C. Parini, "Localisation of body-worn sensors applying ultra wideband technology," *2012 IEEE Asia-Pacific Conf. on Antennas and Propag.*, 106–107, Singapore, 2012.